Atomic Layer Deposition of Al_2O_3 Films on Polyethylene Particles

J. D. Ferguson,[†] A. W. Weimer,[‡] and S. M. George*,[†,‡]

Department of Chemistry and Biochemistry and Department of Chemical and Biological Engineering, University of Colorado, Boulder, Colorado 80309,

Received January 21, 2004. Revised Manuscript Received September 8, 2004

Sequential exposures of $Al(CH_3)_3$ and H_2O at 77 °C were used to encapsulate low-density polyethylene (LDPE) particles with an ultrathin Al_2O_3 film. FTIR studies revealed that the nucleation of Al_2O_3 atomic layer deposition (ALD) on the LDPE particles occurred primarily via adsorption of $Al(CH_3)_3$ onto the LDPE surface or absorption of $Al(CH_3)_3$ into the LDPE particle followed by the reaction with H_2O. The FTIR spectra then revealed the progressive switching between $AlCH_3$* and AlOH* species with alternating exposure to $Al(CH_3)_3$ and H_2O. This nucleation of Al_2O_3 ALD did not require the existence of specific chemical functional groups on the polymer. The FTIR spectra also demonstrated that the sequential exposures of $Al(CH_3)_3$ and H_2O led to an increase in Al_2O_3 bulk vibrational modes. The increase of the absorbance for the Al_2O_3 bulk vibrational modes was linear with the number of AB cycles. The presence of an Al_2O_3 film on the LDPE particles was confirmed using transmission electron microscopy (TEM). The TEM images revealed that the Al_2O_3 coating was very conformal to the LDPE particles. The Al_2O_3 coating was also thicker than expected from typical Al_2O_3 ALD growth rates. This thicker Al_2O_3 coating was explained by the presence of hydrogen-bonded H_2O on the Al_2O_3 surface that increases the Al_2O_3 growth rate during $Al(CH_3)_3$ exposures. On the basis of these results and additional investigations, a model is proposed for Al_2O_3 ALD on polymers. Al_2O_3 ALD should provide an effective gas diffusion barrier on temperature-sensitive polymeric materials such as LDPE.

I. Introduction

Improving polymer properties can benefit the multitude of uses for polymers. The high gas permeability of polymers is one property that limits their use in various food, medical, and electronic packaging applications.[1−3] Inorganic materials typically have a much lower gas permeability than polymers. When used as coatings on polymers, these inorganic materials can serve as gas diffusion barriers and can dramatically improve the polymer performance.[1−3] However, polymers are thermally fragile. Low-temperature deposition techniques such as sputtering, evaporation, and plasma-enhanced chemical vapor deposition have been required to deposit the inorganic diffusion barrier.[3]

Because inorganic materials are brittle, thin inorganic diffusion barriers on polymers are needed to maintain polymer flexibility without cracking. The optimum thickness for maximum flexibility may be as thin as 10−20 nm.[4] For these small thicknesses, line-of-sight deposition techniques such as sputtering and evaporation are limited by defects and pinholes. Atomic layer deposition (ALD) is a chemical vapor deposition (CVD) method based on sequential, self-limiting surface reactions.[5−7] One of the hallmarks of ALD is continuous and pinhole-free deposition. This characteristic is critical for excellent dielectric layers[8] and may also prove important for gas diffusion barriers.

The ALD of many inorganic materials occurs at temperatures >100−200 °C that are higher than the glass-transition temperatures of most polymers. However, the ALD of inorganic materials at low temperature has been demonstrated for several inorganic materials. Catalytic SiO_2 ALD with $SiCl_4$ and H_2O reactants can be accomplished using a Lewis base catalyst at temperatures as low as room temperature.[9−11] Al_2O_3 ALD with $Al(CH_3)_3$ and H_2O reactants can also be achieved at temperatures as low as 33 °C without the use of a catalyst.[12] Both of these ALD processes are compatible with many polymers that have their glass-transition temperatures <200 °C. Al_2O_3 ALD at 177 °C was

* Address correspondence to this author. E-mail: Steven.George@Colorado.edu.
[†] Department of Chemistry and Biochemistry.
[‡] Department of Chemical and Biological Engineering.

(1) Weaver, M. S.; Michalski, L. A.; Rajan, K.; Rothman, M. A.; Silvernail, J. A.; Brown, J. J.; Burrows, P. E.; Graff, G. L.; Gross, M. E.; Martin, P. M.; Hall, M.; Mast, E.; Bonham, C.; Bennett, W.; Zumhoff, M. *Appl. Phys. Lett.* **2002**, *81*, 2929.
(2) Chatham, H. *Surf. Coat. Technol.* **1996**, *78*, 1.
(3) Erlat, A. G.; Spontak, R. J.; Clarke, R. P.; Robinson, T. C.; Haaland, P. D.; Tropsha, Y.; Harvey, N. G.; Vogler, E. A. *J. Phys. Chem. B* **1999**, *103*, 6047.
(4) Yializis, A.; Mikhael, M. G.; Ellwanger, R. E. *43rd Annual Technical Conference Proceedings*; Society of Vacuum Coaters: Albuquerque, NM, 2000; p 404.
(5) Suntola, T. *Thin Solid Films* **1992**, *216*, 84.
(6) George, S. M.; Ott, A. W.; Klaus, J. W. *J. Phys. Chem.* **1996**, *100*, 13121.
(7) Ritala, M.; Leskela, M. Atomic Layer Deposition. In *Handbook of Thin Film Materials*; Academic Press: San Diego, CA, 2001.
(8) Groner, M. D.; Elam, J. W.; Fabreguette, F. H.; George, S. M. *Thin Solid Films* **2002**, *413*, 186.
(9) Klaus, J. W.; Sneh, O.; George, S. M. *Science* **1997**, *278*, 1934.
(10) Klaus, J. W.; Sneh, O.; Ott, A. W.; George, S. M. *Surf. Rev. Lett.* **1999**, *6*, 435.
(11) Klaus, J. W.; George, S. M. *Surf. Sci.* **2000**, *447*, 81.

10.1021/cm040008y CCC: $27.50
Published on Web 12/21/2004

recently demonstrated on SiLK low-k polymer dielectric.[13]

Many polymeric materials are formed using polymer particles.[14] Coating inorganic films on polymer particles offers the possibility to tune the properties of the composite polymer−inorganic materials. A thin inorganic film on the polymer particle can be likened to the "shell on an egg". When the polymer is formed from polymer particles in the extrusion process, the particles are heated and pressed together.[14] During this extrusion, the shell on the egg may crack and disperse the shell fragments throughout the resultant polymer. This high dispersion of cracked shell fragments would offer a very tortuous path for gas molecules diffusing through the polymer.[15,16]

ALD on polymers is complicated by the absence of the necessary chemical functional groups for the ALD surface reactions. Many polymers, such as polyethylene and polypropylene, are saturated hydrocarbons that lack typical chemical functional groups such as hydroxyl (−OH) species. However, Al_2O_3 ALD is remarkably robust and has demonstrated an ability to deposit Al_2O_3 films on nearly every substrate.[12,17−19] Together with its low deposition temperature, the ubiquitous ability of Al_2O_3 to deposit on a variety of substrates led to the judgment that Al_2O_3 ALD was a good candidate for the deposition of inorganic films on polymers.

In this paper, the details of low-temperature Al_2O_3 ALD on polymers are characterized for the first time. Al_2O_3 ALD with $Al(CH_3)_3$ and H_2O reactants was used to deposit Al_2O_3 films on low-density polyethylene (LDPE) particles at 77 °C. The initiation and growth of the Al_2O_3 ALD films was studied using Fourier transform infrared (FTIR) spectroscopy. These FTIR studies allowed the identification of the surface species during the sequential $Al(CH_3)_3$ and H_2O exposures and the progressive growth of the bulk Al_2O_3 film on the LDPE particles. The Al_2O_3 film on the PE particles was also examined using transmission electron microscopy (TEM). These FTIR and TEM studies clarified the growth mechanism during Al_2O_3 ALD on the LDPE particles and characterized the morphology of the Al_2O_3 ALD film.

II. Experimental Section

A vacuum apparatus designed for in-situ transmission FTIR vibrational spectroscopy studies was used to deposit Al_2O_3 on the low-density polyethylene (LDPE) particles. This system has been described previously in detail.[19−22] FTIR spectroscopy provides an effective way to monitor the surface chemistry on the LDPE particles during Al_2O_3 ALD. In brief, the vacuum apparatus consisted of two chambers separated by a gate valve. The FTIR studies were conducted in the upper chamber. Several leak valves and a Baratron capacitance manometer controlled the reactant exposures in the upper chamber. The lower chamber was maintained at high vacuum by a 200 $l\ s^{-1}$ turbomolecular pump. This chamber also contained an ion gauge and a Dycor quadrupole mass spectrometer.

Samples with a high surface area are necessary for transmission FTIR spectroscopy studies. Low-density polyethylene particles were obtained from Equistar Chemicals (Cincinnati, OH). These LDPE particles had an average particle diameter of 2 μm with a diameter range of 1−4 μm. These particles provided a sufficient surface area for the transmission FTIR studies.

The low-density polyethylene particles were supported by a tungsten grid.[19−22] This tungsten grid had 100 lines per inch and was obtained from Buckbee-Mears (St. Paul, MN). The particles were pressed into the grid using polished stainless steel dies and a manual press. A tantalum foil was spot-welded to each side of the grid to facilitate resistive heating. This sample was then suspended between two copper clamps on the sample mount as described previously.[19−22]

The sample mount was attached to an $x-y-z$ rotary manipulator. The $x-y-z$ adjustment capabilities were useful for proper alignment of the sample in the infrared beam. The manipulator also contained current and thermocouple feedthroughs for sample heating and temperature regulation. The vibrational spectroscopic studies were performed with a Nicolet Magna 560 Fourier Transform Infrared (FTIR) spectrometer and MCT-B infrared detector. All of the spectra in this study were recorded with the sample at 77 °C. During reactant exposures, the CsI windows on the chamber were isolated by gate valves to prevent deposition on the windows.

The TEM analysis was performed by Dr. Huifang Xu in the Department of Earth and Planetary Sciences and the Center for Composite and Ceramic Materials at the University of New Mexico. The TEM results were obtained with an HRTEM JEOL 2010 high-resolution transmission electron microscope in combination with electron dispersive spectroscopy and a GATAN digital micrograph with a slow-scan CCD camera. These TEM studies monitored the conformality and morphology of the Al_2O_3 coatings on the LDPE particles.

III. Results and Discussion

Transmission Fourier transform infrared (FTIR) spectroscopy was used to characterize the low-density polyethylene (LDPE) particles. After loading the LDPE particles in the vacuum chamber, the sample was heated to 77 °C. Figure 1 shows an FTIR spectrum of these particles. The predominant features are labeled and are consistent with polyethylene. The features at 2800−3000, 1460, and 720 cm^{-1} are attributed to C−H stretching, deformation, and rocking modes of CH_2 groups.[23]

Sequential exposures of $Al(CH_3)_3$ and H_2O at 77 °C were used to deposit Al_2O_3 on the low-density polyethylene particles. Al_2O_3 ALD film growth proceeds according to two self-limiting surface reactions. The TMA and H_2O exposures yield Al_2O_3 ALD according to the following two reactions:[17,18]

$$\text{(A)}\ Al{-}OH^* + Al(CH_3)_3 \rightarrow Al{-}O{-}Al(CH_3)_2{}^* + CH_4 \quad (1)$$

$$\text{(B)}\ Al{-}CH_3{}^* + H_2O \rightarrow Al{-}OH^* + CH_4 \quad (2)$$

where the asterisks denote the surface species. When performed in an ABAB... reaction sequence, these sequential reactions produce linear, atomic layer con-

(12) Groner, M. D.; Fabreguette, F. H.; Elam, J. W.; George, S. M. *Chem. Mater.* **2004**, *16*, 639.
(13) Elam, J. W.; Wilson, C. A.; Schuisky, M.; Sechrist, Z. A.; George, S. M. *J. Vac. Sci. Technol., B* **2003**, *21*, 1099.
(14) Stevens, M. P. *Polymer Chemistry: An Introduction*; Oxford University Press: New York, 1999.
(15) Gorrasi, G.; Tortora, M.; Vittoria, V.; Pollet, E.; Lepoittevin, B.; Alexandre, M.; Dubois, P. *Polymer* **2003**, *44*, 2271.
(16) Alexandre, M.; Dubois, P. *Mater. Sci. Eng. R.* **2000**, *28*, 1.
(17) Dillon, A. C.; Ott, A. W.; Way, J. D.; George, S. M. *Surf. Sci.* **1995**, *322*, 230.
(18) Ott, A. W.; Klaus, J. W.; Johnson, J. M.; George, S. M. *Thin Solid Films* **1997**, *292*, 135.
(19) Ferguson, J. D.; Weimer, A. W. George, S. M. *Thin Solid Films* **2000**, *371*, 95.
(20) Ferguson, J. D.; Weimer, A. W.; George, S. M. *Thin Solid Films* **2002**, *413*, 16.
(21) Ferguson, J. D.; Weimer, A. W.; George, S. M. *Appl. Surf. Sci.* **2000**, *162*, 280.
(22) Ferguson, J. D.; Weimer, A. W.; George, S. M. *Chem. Mater.* **2000**, *12*, 3472.

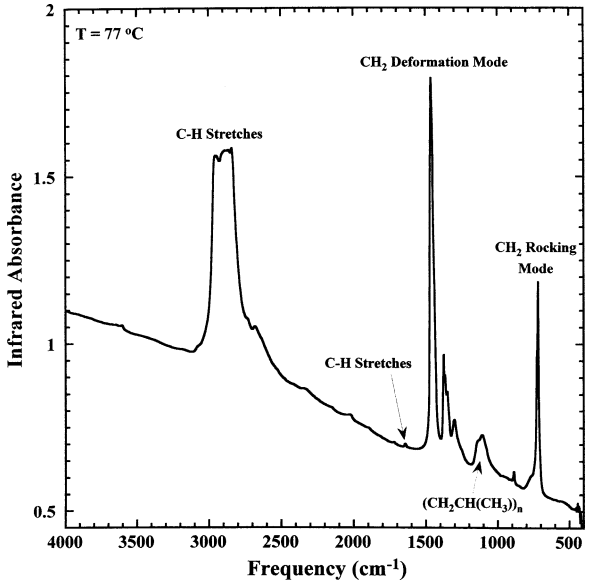

Figure 1. FTIR spectrum of low-density polyethylene (LDPE) particles obtained in a vacuum at 77 °C.

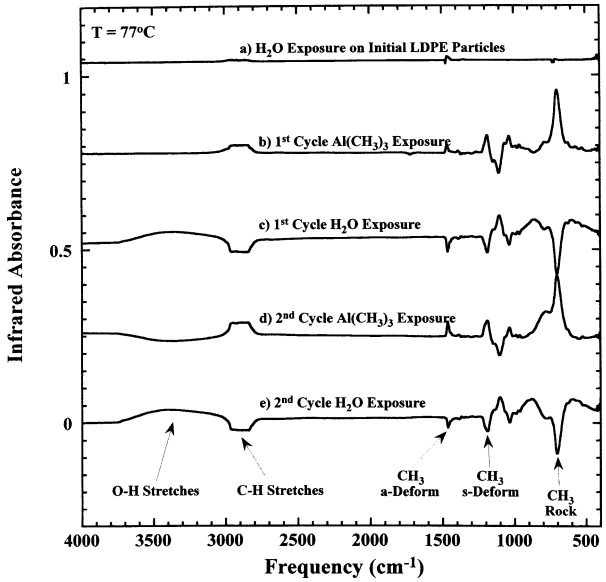

Figure 2. FTIR difference spectra of LDPE particles recorded after (a) H_2O exposure on initial particles, (b) first cycle Al$(CH_3)_3$ exposure, (c) first cycle H_2O exposure, (d) second cycle Al$(CH_3)_3$ exposure, and (e) second cycle H_2O exposure. All exposures and recorded spectra were conducted at 77 °C.

trolled Al_2O_3 growth. Growth rates of 1.1−1.3 Å/cycle have been measured at temperatures from 33 to 177 °C.[12,18]

Atomic layer deposition (ALD) on particles has been demonstrated earlier for a variety of systems including Al_2O_3 ALD on BN particles,[19,21] SiO_2 ALD on BN particles,[21,22] BN ALD on ZrO_2 particles,[20] and TiO_2 ALD on ZrO_2 particles.[24] When the particle surface is covered by the necessary chemical functional groups, such as hydroxyl (−OH) species, ALD yields very smooth, conformal, and atomic layer controlled deposition on the particles. Only SiO_2 ALD on BN particles did not yield conformal deposition because of initial nucleation problems.[21,22]

ALD on a dissimilar material may require a nucleation period. A nucleation period of 8−10 AB reaction cycles was recently observed for W ALD on SiO_2 surfaces.[25] Al_2O_3 ALD is frequently studied on hydroxylated oxide surfaces.[8,26] On these surfaces, Al$(CH_3)_3$ reacts readily with the surface hydroxyl species and Al_2O_3 ALD nucleation usually occurs in the first AB reaction cycle. In contrast, Al_2O_3 ALD nucleation can require 30−40 AB reaction cycles on nonhydroxylated surfaces such as hydrogenated silicon.[26] The nucleation of Al_2O_3 ALD on LDPE may be difficult because of the absence of any hydroxyl species. However, other initiation mechanisms may be operative on porous polymer surfaces.

Figure 2 shows the FTIR difference spectra after the first few Al$(CH_3)_3$ and H_2O exposures. These difference spectra are displaced from the origin for clarity in presentation. Each difference spectrum is referenced to the spectrum recorded immediately before the exposure.

Figure 2a shows the FTIR difference spectrum after the first H_2O exposure at 77 °C on the initial LDPE particles referenced to the spectrum prior to this H_2O exposure. This H_2O exposure of 3.0×10^9 L (1 Langmuir = 1×10^{-6} Torr s) was defined by a H_2O pressure of 5.0 Torr for a period of 10 min.

The difference spectrum in Figure 2a shows that the initial LDPE particles are unreactive to H_2O exposures of 3.0×10^9 L at 77 °C. This behavior is expected since polyethylene is composed of hydrocarbon chains. A strong hydrophobic interaction would be expected between the nonpolar hydrocarbon chains and the polar H_2O molecule. H_2O would not be expected to adsorb strongly onto the LDPE surface or absorb into the bulk of the LDPE particles at 77 °C.

The FTIR difference spectrum taken after the first cycle Al$(CH_3)_3$ exposure at 77 °C is shown in Figure 2b. The Al$(CH_3)_3$ exposure was not conducted until the pressure in the vacuum chamber reached 2.0×10^{-6} Torr after the previous H_2O exposure. This TMA exposure of 1.2×10^9 L was defined by a TMA pressure of 2.0 Torr for a period of 10 min. Many changes are observed in the FTIR difference spectrum in Figure 2b. This spectrum displays the addition of vibrational features at ∼2800−3000, 1467, 1191, and 708 cm^{-1}.

These positive absorbance features are consistent with the vibrational features of molecular Al$(CH_3)_3$. The positive feature at 2800−3000 cm^{-1} is consistent with C−H stretches of Al$(CH_3)_3$.[27,28] The C−H stretches of Al$(CH_3)_3$ usually appear as sharper peaks with frequencies of 2932, 2892, and 2824 cm^{-1}.[28] However, these peaks may be perturbed and obscured by the various C−H vibrational modes and strong C−H absorbance of the LDPE particles. Additional features at 1467, 1191, and 708 cm^{-1} are attributed to the CH_3 asymmetric

(23) Hummel, D. O. *Infrared Analysis of Polymers, Resins and Additives An Atlas*; Wiley-Interscience: New York, 1971.
(24) Ferguson, J. D.; Yoder, A. R.; Weimer, A. W.; George, S. M. *Appl. Surf. Sci.* **2004**, *226*, 393.
(25) Elam, J. W.; Nelson, C. E.; Grubbs, R. K.; George, S. M. *Thin Solid Films* **2001**, *386*, 41.
(26) Tsai, W.; Carter, R. J.; Nohira, H.; Caymax, M.; Conard, T.; Cosnier, W.; DeGendt, S.; Heyns, M.; Petry, J.; Richard, O.; Vandervorst, W.; Young, E.; Zhao, C.; Maes, J.; Tuominen, M.; Schulte, W. H.; Garfunkel, E.; Gustafsson, T. *Microelectron. Eng.* **2003**, *65*, 259.
(27) Gow, T. R.; Lin, R.; Cadwell, L. A.; Lee, F.; Backman, A. L.; Masel, R. I. *Chem. Mater.* **1989**, *1*, 406.
(28) Ogawa, T. *Spectrochim. Acta* **1968**, *24A*, 15.

deformation, CH_3 symmetric deformation, and the CH_3 rocking modes of $Al(CH_3)_3$, respectively.[27,28]

The $Al(CH_3)_3$ exposure at 77 °C also results in negative features in the range of 1080−1170 cm^{-1} and small negative features at 1722 and 1741 cm^{-1}. The absorbance features at 1080−1170 cm^{-1} result from $[CH_2CH(CH_3)]_n$ vibrational modes in the initial LDPE particles.[29] Following the TMA exposures, these absorbance features increase slightly in intensity after very long pumpout times. In addition, these absorbance features reappear after the subsequent H_2O exposure at 77 °C.

The perturbation of the LDPE absorbance features may be explained by the absorption of $Al(CH_3)_3$ into the LDPE particles. The absorption of TMA into the hydrocarbon chains of polyethylene could lead to shifts in frequencies and intensities of various polyethylene vibrational modes associated with $[CH_2CH(CH_3)]_n$ features.[29] These vibrational features are then returned to their initial state after the $Al(CH_3)_3$ molecules are desorbed during long pumpout times or removed by reaction with H_2O. This behavior continues during the first several AB cycles.

The increase in C−H stretching features at ∼2800−3000 cm^{-1} and the perturbation of polyethylene $[CH_2CH(CH_3)]_n$ vibrational features at 1080−1170 cm^{-1} suggests that TMA easily adsorbs on the surface of the LDPE particle and absorbs into the LDPE particle. This adsorption and absorption is expected because $Al(CH_3)_3$ is nonpolar. $Al(CH_3)_3$ should have a reasonable solubility in the nonpolar LDPE particle. $Al(CH_3)_3$ has a high solubility in various nonpolar organic liquids such as benzene.[30]

The small negative features at 1722 and 1741 cm^{-1} are attributed to the removal of oxidized polyethylene species present on the initial LDPE particles.[23] These oxidized polyethylene features do not reappear after the subsequent H_2O exposure or during any of the remaining AB cycles. This behavior is consistent with the first $Al(CH_3)_3$ exposure reacting and permanently removing these oxidized polyethylene species.

The subsequent H_2O exposure of 3.0×10^9 L at 77 °C is shown in Figure 2c. The H_2O exposure was not conducted until the pressure in the vacuum chamber reached 2.0×10^{-6} Torr after the previous $Al(CH_3)_3$ exposure. All of the new features that were added as a result of the previous $Al(CH_3)_3$ exposure are removed by the first cycle H_2O exposure. A broad positive feature in the O−H stretching region is also observed from 3000 to 3700 cm^{-1}. In addition, no infrared absorbance features were observed at ∼1640 cm^{-1} in Figure 2c that would correspond to the H−O−H scissors mode of molecular H_2O.

The lack of a H−O−H scissors mode indicates that the O−H stretching mode at 3000−3700 cm^{-1} corresponds to hydroxyl (−OH) species. The changes observed in Figure 2c are consistent with H_2O reacting with adsorbed and absorbed $Al(CH_3)_3$ and forming $Al(OH)_3$ species. This H_2O reaction could occur as a result of $Al(CH_3)_3$ diffusion out of the LDPE particle to encounter H_2O at the surface. H_2O could also diffuse into the near-surface region of the LDPE particle to react with $Al(CH_3)_3$.

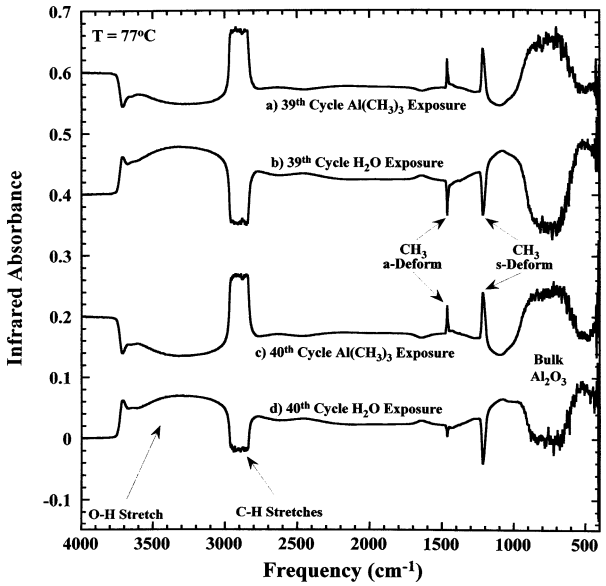

Figure 3. FTIR difference spectra of LDPE particles recorded after (a) 39th cycle $Al(CH_3)_3$ exposure, (b) 39th cycle H_2O exposure, (c) 40th cycle $Al(CH_3)_3$ exposure, and (d) 40th cycle H_2O exposure. All exposures and recorded spectra were conducted at 77 °C.

Figure 2d and 2e displays spectra recorded after the second cycle $Al(CH_3)_3$ and H_2O exposures at 77 °C, respectively. The $Al(CH_3)_3$ exposure was 1.2×10^9 L and the H_2O exposure was 3.0×10^9 L. These exposures were not performed until the vacuum pressure was reduced to 2.0×10^{-6} Torr following the previous exposure. Figure 2d is characterized by positive features consistent with the addition of vibrational features of chemisorbed or molecular $Al(CH_3)_3$ as observed in Figure 2b. In addition, a negative feature in the region of 3000−3700 cm^{-1} is observed in Figure 2d that is consistent with the removal of O−H stretching vibrations. Opposite changes are observed in the spectrum in Figure 2e after the subsequent second cycle H_2O exposure. This behavior is consistent with the addition and removal of $Al(CH_3)_3$ and its reaction products with alternating $Al(CH_3)_3$ and H_2O exposures, respectively.

Figure 3 displays the difference spectra for the 39th and 40th cycle $Al(CH_3)_3$ and H_2O exposures. These are the final two AB cycles conducted by this study. The $Al(CH_3)_3$ exposures were 1.8×10^9 L and the H_2O exposures were 3.0×10^9 L for the 39th and 40th cycles and all the intervening $Al(CH_3)_3$ and H_2O exposures. These exposures also were not performed until the vacuum pressure was reduced to $\leq 2.0 \times 10^{-6}$ Torr following the previous exposure. These difference spectra reveal that the surface species have changed resulting from Al_2O_3 ALD on the LDPE particles.

Figure 3a and 3c shows nearly identical difference spectra recorded after the 39th and 40th cycle $Al(CH_3)_3$ exposures, respectively, at 77 °C. The positive features at 2800−3000, 1464, and 1216 cm^{-1} correspond to the C−H stretching vibrations, the asymmetric CH_3 deformation mode, and the symmetric CH_3 deformation mode, respectively.[27,28] The negative features observed at 3711 and 1640 cm^{-1} are attributed to the O−H stretching vibrations of isolated AlOH* species on Al_2O_3

(29) Bark, L. S., Allen, N. S., Eds., *Analysis of Polymer Systems*; Applied Science Publishers Ltd.: London, 1982.
(30) Lasserre, S.; Derouault, J. *New J. Chem.* **1983**, *7*, 659.

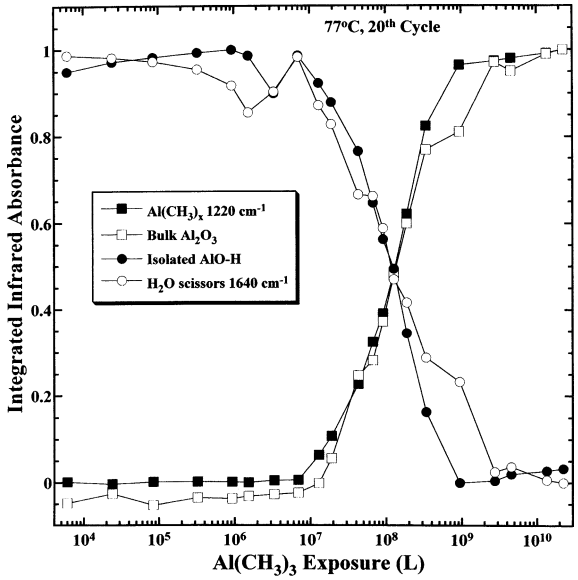

Figure 4. Normalized integrated absorbance of the CH_3 symmetric deformation mode at 1220 cm^{-1}, the isolated O−H stretching vibrational mode at 3716 cm^{-1}, the H_2O scissors mode at 1640 cm^{-1}, and the Al_2O_3 bulk vibrational mode versus $Al(CH_3)_3$ exposure during the 20th reaction cycle at 77 °C.

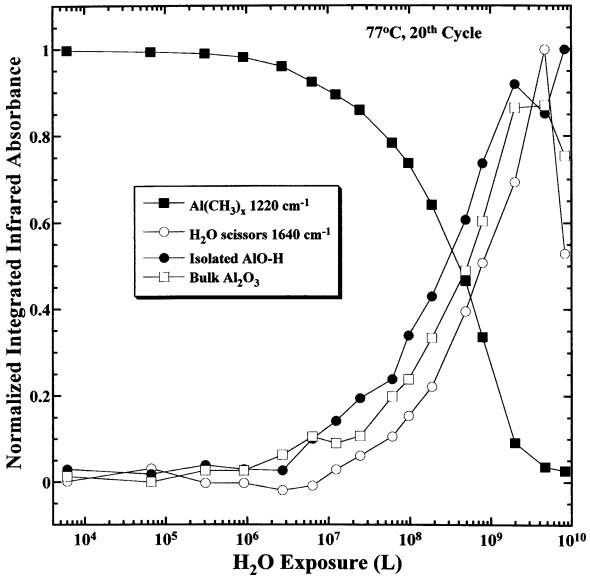

Figure 5. Normalized integrated absorbance of the CH_3 symmetric deformation mode at 1220 cm^{-1}, the isolated O−H stretching vibrational mode at 3716 cm^{-1}, the H_2O scissors mode at 1640 cm^{-1}, and the Al_2O_3 bulk vibrational mode versus H_2O exposure during the 20th reaction cycle at 77 °C.

surfaces and the scissors mode of hydrogen-bonded H_2O. An additional negative feature in the range of 3000−3700 cm^{-1} is attributed to a combination of O−H stretches from hydrogen-bonded AlOH* surface species and from hydrogen-bonded H_2O.

Figure 3b and 3d shows the difference spectra taken after the 39th and 40th cycle H_2O exposures, respectively, at 77 °C. These spectra are nearly identical to each other and mirror images of the difference spectra shown in Figure 3a and 3c. This behavior is consistent with $Al(CH_3)_3$ exposures reacting with both AlOH* species and hydrogen-bonded H_2O to form $AlCH_3$* species. The subsequent H_2O exposures then react with the $AlCH_3$* species to form AlOH* species. Additional H_2O undergoes hydrogen-bonding to the newly formed AlOH* species. The scissors mode of hydrogen-bonded H_2O appears as a positive feature at 1640 cm^{-1}.

The bulk Al_2O_3 vibrational modes appear in Figure 3 at <1000 cm^{-1}.[19] The difference spectra display a gain of absorbance for the bulk Al_2O_3 mode after $Al(CH_3)_3$ exposures and a loss of absorbance for the bulk Al_2O_3 mode after H_2O exposures. However, this bulk Al_2O_3 vibrational mode grows steadily with the number of AB reaction cycles as will be demonstrated below.

Figures 4 and 5 display the reactive adsorption of $Al(CH_3)_3$ and H_2O, respectively, during the 20th AB cycle at 77 °C. The $AlCH_3$* surface species were monitored using the CH_3 symmetric deformation mode at 1220 cm^{-1}.[27] The O−H stretch at 3716 cm^{-1} was used to monitor the isolated AlOH* surface species. The H_2O scissors mode at 1640 cm^{-1} was used to monitor the hydrogen-bonded water. Additionally, the growth of Al_2O_3 was monitored by its bulk vibrational mode. The bulk Al_2O_3 vibrational mode was measured by integrating over the infrared region from 450 to 1050 cm^{-1}.

Figure 4 shows the integrated absorbances of various vibrational features versus $Al(CH_3)_3$ exposure at 77 °C. The CH_3 symmetric deformation mode at 1220 cm^{-1} and the Al_2O_3 bulk vibrational mode at 450−1050 cm^{-1} increase and then level off with increasing $Al(CH_3)_3$ exposure. Concurrently, the O−H stretching vibrational mode and the H_2O scissors mode decrease and then level off with increasing $Al(CH_3)_3$ exposure. On the basis of these and previous results, $Al(CH_3)_3$ exposures of $\geq 1.8 \times 10^9$ L were used to ensure the completion of the $Al(CH_3)_3$ reaction.

The integrated absorbances of the same vibrational features are plotted versus H_2O exposure at 77 °C in Figure 5. The CH_3 symmetric deformation mode at 1220 cm^{-1} decreases and levels off with increasing H_2O exposure. The O−H stretching vibrational mode, the H_2O scissors mode, and the Al_2O_3 bulk vibrational mode at 450−1050 cm^{-1} all increase and then level off with increasing H_2O exposure. On the basis of these and previous results, H_2O exposures of $\geq 3.0 \times 10^9$ L were used to ensure the completion of the H_2O reaction. The integrated absorbance of the H_2O scissors mode and the isolated AlO−H stretching vibration were dependent upon the evacuation time after the H_2O exposure prior to recording the FTIR spectrum. This behavior is attributed to the slow desorption of hydrogen-bonded H_2O from the hydroxylated Al_2O_3 surface.

The TMA and H_2O exposures required for complete reactions were $\geq 1.8 \times 10^9$ L and $\geq 3.0 \times 10^9$ L, respectively. These exposures are much longer than the exposures of $\sim 1 \times 10^4 - 1 \times 10^5$ L measured in previous studies.[18,31] These long exposures are required by the low conductance of the reactants to the surface species. The low conductance is believed to result from pressing the easily deformable polymer particles into the tungsten grid. The pressure on the particles presumably removes the gaps between the particles and lowers the gas conductance through the polymer particle bed. Much smaller exposures are expected for flat polymer substrates in a viscous flow reactor[31] or polymer particles in a fluidized particle bed.[32]

(31) Elam, J. W.; Groner, M. D.; George, S. M. *Rev. Sci. Instrum.* **2002**, *73*, 2981.

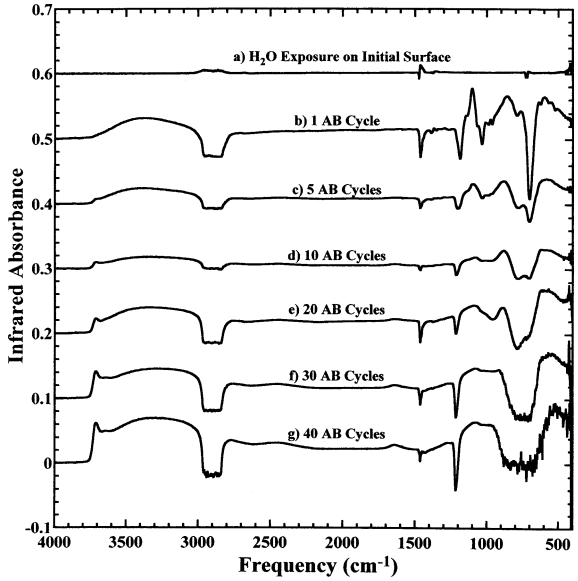

Figure 6. FTIR difference spectra of the LDPE particles after various AB cycles at 77 °C ending with the H_2O exposure. Each spectrum is referenced to the spectrum recorded prior to the H_2O exposure.

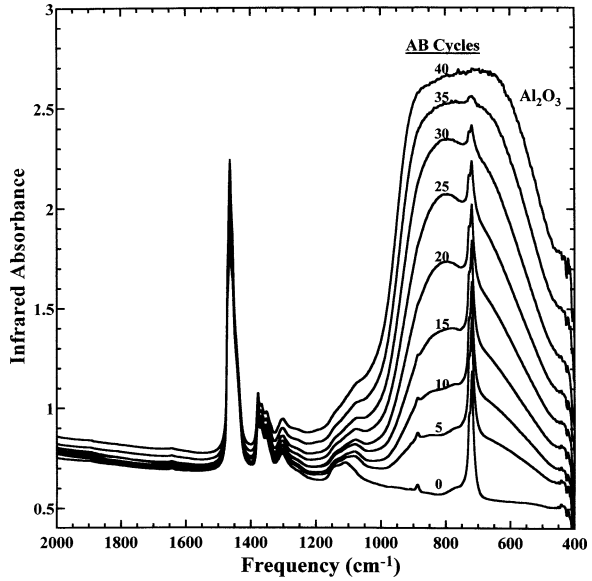

Figure 7. FTIR spectra showing the growth of Al_2O_3 bulk vibrational modes at 400−1100 cm^{-1} versus the number of AB reaction cycles at 77 °C.

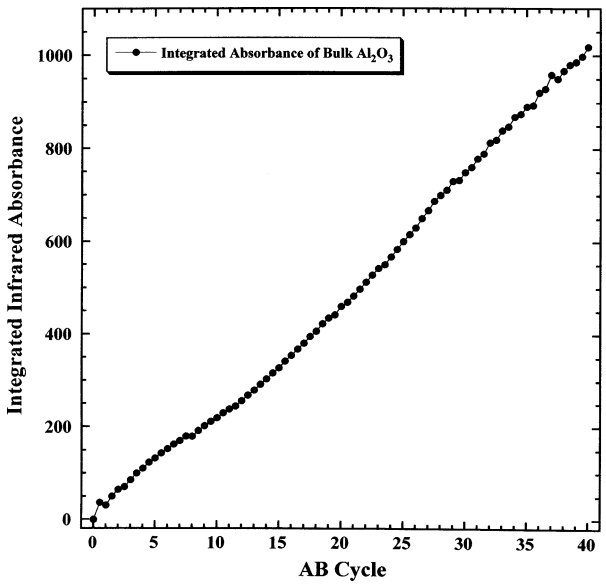

Figure 8. Integrated absorbance of the Al_2O_3 bulk vibrational modes at 400−1100 cm^{-1} versus the number of AB reaction cycles at 77 °C.

Figure 6 shows the difference spectra recorded after the H_2O exposures for various AB reaction cycles at 77 °C. The difference spectrum shown in Figure 6a was recorded after the first H_2O exposure on the initial LDPE particles and shows almost no change relative to the spectrum for the initial LDPE particles. The subsequent spectra show positive absorbance features in the O−H stretching region and a negative absorbance feature in the C−H stretching region. The initial surface of the particles consists of low-density polyethylene. As Al_2O_3 is deposited through the repetition of the $Al(CH_3)_3$ and H_2O exposures at 77 °C, the surface evolves to an Al_2O_3 surface.

Figure 6 reveals that a sharp peak at 3711 cm^{-1} emerges as a function of the number of $Al(CH_3)_3/H_2O$ reaction cycles. This sharp peak is attributed to the O−H stretching vibration of an isolated AlOH* species on an Al_2O_3 surface.[17,33] This feature indicates that small Al_2O_3 clusters have formed and yield characteristic isolated AlOH* species by the fifth AB cycle. The difference spectra in Figure 6 also reveal the presence of more hydrogen-bonded H_2O molecules at 1640 cm^{-1} with increasing number of AB reaction cycles. Since H_2O did not adsorb on the LDPE surface or absorb into the initial LDPE particles, this hydrogen-bonding of H_2O is characteristic of the presence of a hydroxylated Al_2O_3 surface. The H_2O scissors mode is visible after 5 AB cycles and distinct after 10 AB cycles.

The growth of the bulk Al_2O_3 vibrational mode on the LDPE particles was also observed by the FTIR spectra. An increase in the intensity of the bulk Al_2O_3 vibrational modes at 400−1100 cm^{-1} was monitored with increasing number of AB reaction cycles at 77 °C. The absolute FTIR spectra after every five AB cycles after the H_2O exposure are shown in Figure 7. The absorbance increases very progressively with the number of AB reaction cycles.

The integrated absorbance of the Al_2O_3 bulk vibrational mode at 400−1100 cm^{-1} is plotted versus the number of AB cycles in Figure 8. The intensity of the Al_2O_3 bulk vibrational mode is nearly linear with the number of AB cycles. This linear growth is expected during Al_2O_3 ALD.[18] This linearity is a characteristic signature of ALD and has been observed previously in numerous studies of Al_2O_3 ALD.[6,18,31,34]

Transmission electron microscopy (TEM) was also used to evaluate the Al_2O_3 films on the LDPE particles. Figure 9 shows a TEM image of an Al_2O_3 film on an LDPE particle. This Al_2O_3 ALD coating was achieved by exposing the LDPE particles to 40 $Al(CH_3)_3/H_2O$ reac-

(32) Wank, J. R.; George, S. M.; Weimer, A. W. *Powder Technol.* **2004**, *142*, 59.

(33) Chen, J. G.; Crowell, J. E.; Yates, J. T. *J. Chem. Phys.* **1986**, *84*, 5906.

(34) Elam, J. W.; Sechrist, Z. A.; George, S. M. *Thin Solid Films* **2002**, *413*, 43.

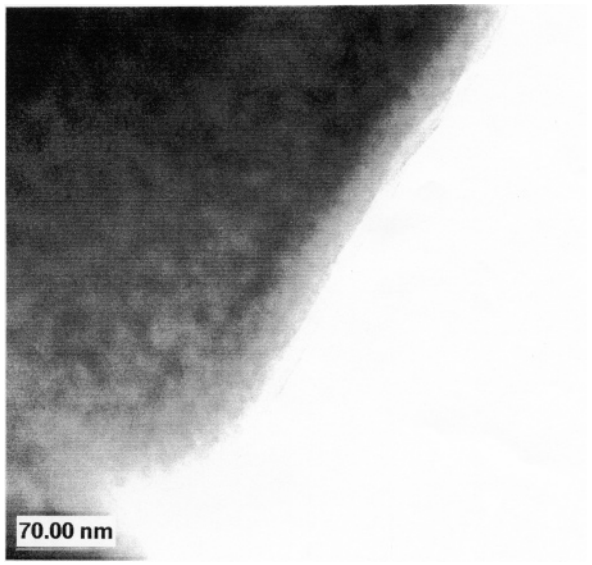

Figure 9. Transmission electron microscope image of an LDPE particle after 40 $Al(CH_3)_3/H_2O$ reaction cycles at 77 °C. The thickness of the conformal and amorphous Al_2O_3 ALD film varies from 130 to 180 Å.

tion cycles at 77 °C. These were the same 40 AB reaction cycles that were utilized for the FTIR experiments.

The Al_2O_3 film is very smooth and conformal on the LDPE particles. Similar results were observed for Al_2O_3 ALD on SiLK low-k polymer dielectric.[13] The Al_2O_3 ALD film is also amorphous. The approximate thickness of the Al_2O_3 film varies from 130 to 180 Å after 40 AB cycles. These results yield an Al_2O_3 ALD growth rate of 3.3−4.5 Å/cycle. The observed thickness is larger than the expected thickness of 50 Å for 40 AB cycles predicted by an Al_2O_3 growth rate of 1.25 Å/cycle at 80 °C.[12]

The larger thickness and higher Al_2O_3 growth rate may be explained by the presence of hydrogen-bonded H_2O on the Al_2O_3 surface. This hydrogen-bonded H_2O is measured by the H_2O scissors mode at 1640 cm^{-1}. This H_2O can react with $Al(CH_3)_3$ to deposit additional Al_2O_3 by chemical vapor deposition (CVD). On the basis of the expected Al_2O_3 ALD growth rate of 1.25 Å/cycle at 80 °C, the Al_2O_3 CVD growth rate is determined to be 2.0−3.3 Å/cycle. The existence of the hydrogen-bonded H_2O is attributed to the low conductance for H_2O between the LDPE particles pressed into the tungsten grid.

The adsorption of $Al(CH_3)_3$ onto the LDPE surface and the absorption of $Al(CH_3)_3$ into the LDPE particle is necessary for the nucleation of Al_2O_3 ALD on LDPE. This $Al(CH_3)_3$ uptake may be facilitated by the presence of a low-density, more highly disordered interfacial layer at the surface of the LDPE particles. Monte Carlo simulations reveal much lower densities and higher diffusivities at the surface of amorphous polyethylene.[35] Earlier molecular dynamics simulations also observed lower densities and a "dynamic interfacial layer" on a free surface of glassy atactic polypropylene.[36] Monte Carlo simulations of *n*-alkane molecular crystals have revealed very pronounced disorder within two to three molecular layers of the surface.[37] Thermal probe atomic force microscope studies also observe significantly lower glass-transistion temperatures on the surface of bulk polystyrene.[38]

$Al(CH_3)_3$ adsorption and absorption by this low-density, more highly disordered interfacial layer may promote Al_2O_3 growth in the absence of specific chemical species that can react with $Al(CH_3)_3$. This adsorbed and absorbed $Al(CH_3)_3$ could then react with H_2O during the next H_2O exposure to form $Al(OH)_3$ species. Subsequent TMA exposures could react with $Al(OH)_3$ species and form $Al[OAl(CH_3)_2]$ species. Successive H_2O and TMA exposures could continue to grow Al_2O_3 clusters that are believed to merge and eventually to form a continuous Al_2O_3 film.

The Al_2O_3 ALD film should form an effective gas diffusion barrier after several AB reaction cycles. After the formation of a diffusion barrier, TMA should no longer absorb into the near-surface region of the LDPE polymer. Al_2O_3 ALD should then be dependent only on the TMA reaction with AlOH* and hydrogen-bonded H_2O on the Al_2O_3 surface. The diffusion of $Al(CH_3)_3$ into polyethylene during Al_2O_3 ALD is currently being examined in additional studies by spin-coating a polyethylene film onto a quartz crystal microbalance (QCM) sensor.[39] These QCM experiments allow the mass of the adsorbed $Al(CH_3)_3$ and deposited Al_2O_3 to be measured versus the number of AB reaction cycles.[13] These QCM measurements of Al_2O_3 ALD growth are consistent with porous polyethylene films that absorb TMA until an Al_2O_3 ALD gas diffusion barrier is formed after 20−25 AB cycles.[39]

These FTIR and TEM investigations, together with the additional QCM investigations[39] and earlier studies of Al_2O_3 ALD on SiLK low-k dielectric polymeric films,[13] suggest the following picture for Al_2O_3 ALD on LDPE particles. $Al(CH_3)_3$ initially adsorbs onto the LDPE surface and absorbs into the LDPE particle. The H_2O then reacts with $Al(CH_3)_3$ on the surface and in the near-surface region of the LDPE particle. This reaction produces $Al(OH)_3$ and subsequently small Al_2O_3 clusters after multiple AB cycles. These Al_2O_3 clusters are presumably entangled with the polymer chains. These Al_2O_3 clusters grow with sequential $Al(CH_3)_3$ and H_2O exposures and eventually merge to create a continuous Al_2O_3 film that is an effective gas diffusion barrier. The Al_2O_3 ALD film then grows on the Al_2O_3 coating on the LDPE particle.

Al_2O_3 ALD should be very useful as a gas diffusion barrier on polymers for numerous packaging applications in the food, medical, and electronic fields. The conformality and continuous, pinhole-free character of ALD films should be ideal for high-quality gas diffusion barriers. The atomic layer control achievable with ALD should also allow precise and conformal thicknesses to be deposited on polymeric substrates. Ultrathin inorganic films are important for flexibility without cracking under deformation. Inorganic film thicknesses <20 nm may be needed to maintain optimum flexibility without cracking.[4]

(35) Doruker, P.; Mattice, W. L. *Macromolecules* **1999**, *32*, 194.
(36) Mansfield, K. F.; Theodorou, D. N. *Macromolecules* **1991**, *24*, 6283.
(37) Yamamoto, T.; Hikosaka, M.; Takahashi, N. *Macromolecules* **1994**, *27*, 1466.
(38) Fischer, H. *Macromolecules* **2002**, *35*, 3592.
(39) Wilson, C. A.; Grubbs, R. K.; George, S. M. Department of Chemistry and Biochemistry, University of Colorado, Boulder, Colorado 80309. Unpublished results, 2004.

Al_2O_3 ALD is accomplished using $Al(CH_3)_3$ and H_2O reactants.[6,12,17−19] Other aluminum and oxygen precursors have also been utilized for thermal Al_2O_3 ALD.[40−43] Plasma-enhanced ALD (PEALD) can be used to achieve lower deposition temperatures. Recent studies have reported the PEALD of Al_2O_3 on polyethersulfone (PES) at temperatures ranging from 90 to 150 °C.[44] Although Al_2O_3 ALD was performed at 77 °C in the current paper, the H_2O purge times were long. H_2O purge times of 20 s were needed at 80 °C for Al_2O_3 ALD in a viscous flow ALD reactor.[12] PEALD of Al_2O_3 using O_2 as the oxygen plasma reactant would significantly reduce this purge time.

IV. Conclusions

Al_2O_3 films were grown on low-density polyethylene (LDPE) particles at 77 °C by atomic layer deposition (ALD) using sequential exposures of $Al(CH_3)_3$ and H_2O. Transmission Fourier transform infrared (FTIR) spectroscopy was used to monitor the sequential surface chemistry on the LDPE particles. The FTIR spectra revealed that the initiation of Al_2O_3 ALD on the LDPE particles occurred through the adsorption of $Al(CH_3)_3$ onto the LDPE surface or absorption of $Al(CH_3)_3$ into the porous LDPE particle and subsequent reaction with H_2O. Alternating $Al(CH_3)_3$ and H_2O exposures in an ABAB... reaction sequence produced $AlCH_3$* and AlOH* species, respectively. These AB reactions also yielded Al_2O_3 clusters that were presumably entangled in the polymer chain. The Al_2O_3 clusters are believed to grow and eventually merge to form a continuous Al_2O_3 film that serves as an effective gas diffusion barrier.

The repetition of the $Al(CH_3)_3$ and H_2O exposures led to the linear growth of the vibrational modes for bulk Al_2O_3. Following 40 AB reaction cycles at 77 °C, the LDPE particles were examined using transmission electron microscopy (TEM). These TEM studies revealed that the LDPE particles were encapsulated with conformal amorphous Al_2O_3 coatings. The film thicknesses measured by TEM were larger than expected from earlier studies of Al_2O_3 ALD on flat, nonporous substrates. This larger Al_2O_3 growth rate was attributed to the presence of hydrogen-bonded H_2O resulting from the low conductance between the LDPE particles. This hydrogen-bonded H_2O may lead to a small amount of Al_2O_3 chemical vapor deposition (CVD) that adds to the Al_2O_3 ALD. This study illustrates that specific chemical species on the LDPE surface or LDPE bulk are not needed to initiate Al_2O_3 ALD. This low-temperature ALD technique for depositing Al_2O_3 films on polymer materials should prove very useful for many applications.

Acknowledgment. The authors thank Edward S. Vargas at Equistar Chemicals in Cincinnati, Ohio for providing the low-density polyethylene particles used in these experiments. Some equipment used for the FTIR investigations was provided by support from the Air Force Office of Scientific Research.

CM040008Y

(40) Kumagai, H.; Toyoda, K. *Appl. Surf. Sci.***1994**, *82−3*, 481.
(41) Kukli, K.; Ritala, M.; Leskela, M.; Jokinen, J. *J. Vac. Sci. Technol., A* **1997**, *15*, 2214.
(42) Raisanen, P. I.; Ritala, M.; Leskela, M. *J. Mater. Chem.* **2002**, *12*, 1415.
(43) Cho, W.; Sung, K.; An, K. S.; Lee, S. S.; Chung, T. M.; Kim, Y. *J. Vac. Sci. Technol., A* **2003**, *21*, 1366.
(44) Yun, S. J.; Lim, J. W.; Lee, J. H. *Electrochem. Solid State Lett.* **2004**, *7*, C13.